**Proceedings of 2004 IEEE/RSJ International Conference on Intelligent Robots and Systems
September 28 - October 2, 2004, Sendai, Japan**

Passive Running of Planar 1/2/4-Legged Robots

Sang-Ho Hyon Xin Jiang Takashi Emura
Department of Bioengineering and Robotics
Tohoku University
Sendai 980-8579, Japan
Email: sangho@ieee.org

Tetsushi Ueta
Center for Advanced Information Technology
Tokushima University
Tokushima 770-8506, Japan
Email: tetsushi@is.tokushima-u.ac.jp

***Abstract*— In this paper, we report on passive running of planar one-legged, biped, and quadruped robots. The topic includes the analysis of passive running gaits and their orbital stabilization. For one-legged robot, two stabilizing controllers that asymptotically stabilize periodic passive gaits are derived. In particular, the second controller is based on "energy-preserving principle" and its original form generates interesting quasi-periodic running gaits, which can be seen in Hamiltonian system. The controller is extend to a planar biped robot with torso, which does not have any passive running gaits. Combining simple attitude controller at stance phase generates stable periodic running gaits. For a planar quadruped robot, with an advanced gait searching algorithm, some fundamental proterties of the passive running gaits, such as stability or symmetry, are observed.**

I. INTRODUCTION

After the Raibert's excellent works [1], running robots have been widely studied both experimentally [2][3][4][5] and theoretically [6][7][8]. In the fast running control, energy-efficiency is especially crucial for autonomous robots (including biped humanoid robots or quadruped robots) because it directly extends their operation time. In this connection, there are some remarkable researches on passive running, where the passive running means "unforced" periodic running. Tompson and Raibert showed that spring-driven one-legged hopping robot can hop without any inputs, provided if the initial conditions were appropriately chosen [9]. Ahmadi and Buehler applied Raibert's algorithm to this robot and realized energy-efficient hopping in simulation and experiment [10][11]. François and Samson derived a rather systematic controller based on linearization of the periodic orbit [12].

In this paper, we report on our research motivated from the above works: passive running of planar one-legged, biped, and quadruped robots. The robots are installed with linear springs at the telescopic knee joints and torsional springs at the hip joints. These springs assign strong passive dynamics to the robots. Doing so, we expect the robot exhibits passive periodic running gaits for appropriately chosen parameters and initial conditions.

However, it is almost impossible to obtain analytical solution even for simple 2 DOF case [7]. Threfore the solution can be found numerically. If we can "luckily" find the passive gaits, the next stage is their stability analysis. Even if they are unstable, when the system has some controllability, we can design the controllers, which asymptotically stabilize the gaits. This is a stabilization problem of nonlinear hybrid oscillator, which has not been well discussed. Thus obtained limit cycle is utmost important for energy-efficient locomotion because it does not require any control input when the solution lies on the limit cycle. Moreover, if the controller extends the region of attraction, it directly links to the application to more realistic robot models. If we cannot find any passive gaits unfortunately, we can find some controllers that generate stable limit cycle, in some cases.

Our approach to the analysis and control of passive running robots is different from previous studies in the following sense:

1) We do not rely on some approximations or linearized equations
2) We do not assume the leg has neglgible mass, and consider the impact between the leg and the ground
3) We design feedback controllers based on "energy-preserving principle"

The first point is important for stability analysis and for generation of control inputs that converge to zero when stabilization is achieved. Otherwise, we will have steady-state error. The second point is to reveal the true behavior, which the real robot exhibits. In a simple model, many literature neglect the mass of the leg, and hence, the impact between the foot and the ground. Mass-less leg hides the behavior of the counter-oscillation of the body, and exclusion of impact phenomenon leads to incorrect stability analysis and the controller design. The third point is to derive energy-efficient controllers: energy-preservation is the essential necessary condition of stable passive running.

We will show the above approach by three specific examples; planar one-legged, biped, and quadruped running robots. In Section II, the analysis and control of a passive one-legged running robot is provided. With new results on stability analysis, a local feedback controller is derived and our previously derived stabilization controller, which asymptotically stabilize unknown (multi) periodic passive gaits, is discussed.

Section III extends the controller of one-legged model to a planar biped model having a torso. This biped model is the example that any passive gaits are not found. Combining a simple attitude controller at stance phase, we try to stabilize unknown periodic biped running gaits.

Section IV shows numerical search on passive running gaits of planar quadruped robot. Planar quadruped running is composed of several phases and this complicates the gait analysis. To this end, numerical algorithm in one-legged model is modified. We show two interesting passive running gaits and their properties.

II. One-legged running robot

A. Model

We consider one-legged passive running robot shown in Fig. 1. The robot is attached with not only a leg spring but also a hip spring. The generalized coordinates are defined as the position of center of gravity (CoG) (x, z), the leg length r, and the attitude of the body and the leg (ϕ, θ). The control inputs are the leg force f and hip torque τ. These are applied parallel to the springs. Table I shows the physical parameters, together with the values used for numerical analysis.

The following assumptions are imposed on the model:

(A) Mass of the foot (unsprung mass) is negligible
(B) The foot does not bounce back, nor slip the ground (inelastic impulsive impact)
(C) The springs are mass-less and non-dissipating

Assumption (A) means the foot of the robot is mass-less, and hence, there is no inertial force due to the foot mass. Of course, this assumption cannot be satisfied exactly in real machine, but it is rather easy to make foot lightweight because the foot is a simple rod. Thanks to this assumption, there is no impulse along the leg axis.

On the other hand, when the robot receives the impact of perpendicular direction to the longitudinal axis of the leg, energy less occurs due to the inertia of "upper part" of the leg. If the foot is too repulsive, it may bounce back due to this impulse and the robot cannot touchdown the ground appropriately. However, for our robot, it is easy to make the foot lightweight, its restitution low. More importantly, our controller minimizes touchdown impulse normal to the longitudinal axis of the leg, as shown later. Therefore, assumption (B) on inelastic impulse model represents touchdown dynamics of our one-legged robot most effectively. Assumption (C) is not restrictive one because it is easy to compensate energy loss by applying leg force f.

The equations of motion are presented in [13]. A running motion is composed of successive phase transitions; Stance $\rightarrow$ Flight $\rightarrow$ Stance $\rightarrow \cdots$. Between Stance and Flight, thre are discrete events; Touchdown and Lift-off. Table II defines the phase-indicating subscripts for variables. For example, $\dot{x}_{lo}$ is the forward velocity of C.M. at Lift-off, $\dot{\theta}_{td+}$ is the angular velocity of the leg just before Touchdown, θ_{td} is the leg angle of just before, or, just after Touchdown, and so on.

B. Passive running gaits

To search the passive running gait, Poincaré map is constructed because the existence of the fixed point of Poincaré map means that of passive running gait. To find the fixed points, the Newton-Raphson method is employed as follows.

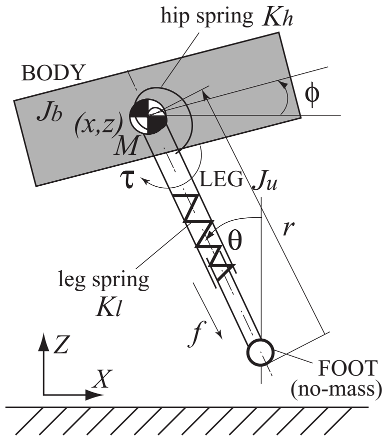

Fig. 1. Passive one-legged hopper

TABLE I
PHYSICAL PARAMETERS OF ONE-LEGGED MODEL

	Meaning	Unit	Value
g	gravity acceleration	$\mathrm{m/s^2}$	9.8
M	total mass	kg	12
r_0	natural leg length	m	0.5
J_b	body inertia	$\mathrm{kgm^2}$	0.5
J_l	equivalent leg inertia	$\mathrm{kgm^2}$	0.11
K_l	leg spring stiffness	N/m	3000
K_h	hip spring stiffness	Nm/rad	10

With the state variable $\underline{x} = [x,\ \theta,\ \phi,\ \dot{x},\ \dot{z},\ \dot{\theta},\ \dot{\phi}]^T$ and the cross section $h(\underline{x}) := z - r_0 \sin\theta = 0$ (just after Touchdown), the Poincaré map can be represented as:

$$\underline{x}_{n+1} = P(\underline{x}_n), \tag{1}$$

where n is the number of strides. We want to find a solution $\underline{x}$ of (1) that maps onto itself, i.e. a solution satisfies the equation:

$$G(\underline{x}) = \underline{x} - P(\underline{x}) = 0 \tag{2}$$

The search space is 7-dimensional. We use Newton-Raphson method for root seeking, where an initial guess for the fixed point is given and then updated based on the following scheme.

For small changes in the state variables, the change in P is approximated by its Taylor series,

$$P(\underline{x} + \Delta\underline{x}) = P(\underline{x}) + DP(\underline{x})\Delta\underline{x} + O(\underline{x}), \tag{3}$$

where $DP(\underline{x}) = \frac{\partial P(\underline{x})}{\partial \underline{x}}$ and $O(\underline{x})$ represents higher order term.

TABLE II
PHASE-INDICATING SUBSCRIPTS

Subscript	Meaning
td-	just before Touchdown
td+	just after Touchdown
td	just before, or after Touchdown
lo	Lift-off

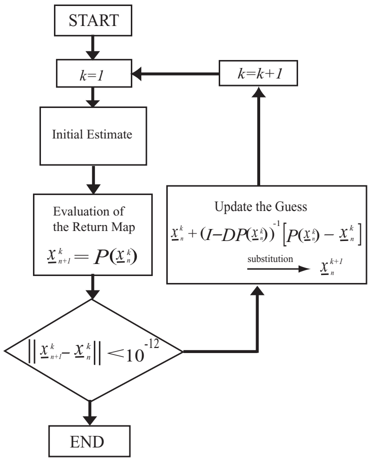

Fig. 2. Gait searching algorithm

Therefore, we have

$$\begin{aligned} &DG(\underline{x})\Delta\underline{x} = -G(\underline{x}) \\ &\Rightarrow \Delta\underline{x} = (\mathbf{I} - DP(\underline{x}))^{-1}(P(\underline{x}) - \underline{x}), \end{aligned} \quad (4)$$

where $\underline{x}$ is the value of the states of the return map calculated at the n^{th} stride. Therefore, we have the following update scheme with a given initial guess $\underline{x}^0$,

$$\underline{x}^{k+1} = \underline{x}^k + (\mathbf{I} - DP(\underline{x}^k))^{-1}(P(\underline{x}^n) - \underline{x}^n), \quad (5)$$

where the index k corresponds to the number of iterations.

The algorithm is summarized in Fig. 2. Note that in addition to the solution $\underline{x}(t)$, DP should also be calculated numerically. Also, if there are jump in the solution $\underline{x}$ due to the impact, DP also should be processed accordingly. See [14] for the details.

For the one-legged model, this algorithm converges rapidly, and we can obtain multiple passive running gaits. The solutions exist for every admissible initial condition and they are actually loss-less, i.e. no energy is dissipated.

For example, a fixed point $\underline{x}$ = [−0.3129, 0.6763, −0.1198, 5.0000, −2.0760, −5.2004, 1.2818] corresponding to high speed passive running as shown in Fig. 3. Its stability can be found from the eigenvalue of DP. In this case $\mathrm{eig}(DP)$ = [−5.6574, 2.0839, −0.1800, 0.0070, 0.0000, 0.0000, 0.0000]. Since the first two elements lie outside the unit circle on the complex plane, we can conclude the passive gait is orbitally unstable. All the other solutions are found to be unstable, except for trivial vertical hopping.

C. Local stabilization by linear feedback

Having obtained passive gaits and checked their stability, we should find appropriate stabilizing controller. Here we show two kinds of controllers in the sequel.

The first one is local stabilization by linear feedback controller. In the above example, we have two unstable manifolds regarding above two unstable eigenvalues. For example, we can apply control input τ at the flight phase:

$$\tau = \begin{cases} \tau_1, & \text{if } \ 0 \le t < T_v/2 \\ \tau_2, & \text{if } \ T_v/2 \le t < T_v \end{cases} \quad (6)$$

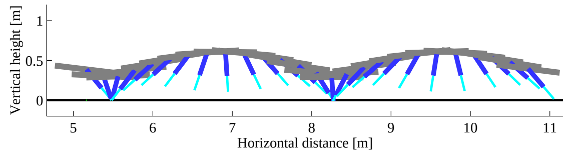

Fig. 3. Subsequent two steps of 1-periodic passive running gait. Running speed is 5 m/s. The robot moves from left to the right.

, where τ_1 and τ_2 are constant values, t is the time after the lift-off, and $T_v := 2\dot{x}_{lo}/g$ means "expected" flight time. Then, we obtain the closed loop system that is stabilizable:

$$\underline{x}_{n+1} = DP_{\underline{x}}\underline{x}_n + DP_u \begin{bmatrix} \tau_1 \\ \tau_2 \end{bmatrix}, \quad (7)$$

where $DP_{\underline{x}}$ is the same as DP in the previous section and $DP_u = \frac{\partial P}{\partial u} = (\frac{\partial P}{\partial \tau_1}, \frac{\partial P}{\partial \tau_2})$ is newly appeared derivative by introducing control input (6).

If we place the two unstable pole to zero, we can stabilize all of the unstable passive gaits obtained in the previous section. However, the region of attraction is found to be quite narrow because the controller is local. Actually, it is found by simulation that the local controller does not allow even 0.05 m/s error in initial velocity $\dot{x}_0$.

D. Stabilization based on energy-preserving principle

We show an alternative controller based on its energy analysis, firstly proposed in [15]. The underlining principle is *energy-preservation*. This means the controller preserves system energy as much as possible. The most important reason why we use this principle is; if the system energy is preserved, it is expected that the system autonomously generate natural periodic gaits, just as some class of Hamiltonian system exhibit natural periodic orbit. Instead of depending on some pre-calculated periodic solutions, or target (desired) dynamics, analysis on energy change of the original nonlinear hybrid system are utilized as shown below.

First, we choose desired touchdown angle θ_d and angular velocity $\dot{\theta}_d$ at the moment of lift-off to meet the following *energy non-dissipation condition*:

$$\mu_{td-} := \dot{x}_{td-}\cos\theta_{td} + \dot{z}_{td-}\sin\theta_{td} + r_0 = \dot{\theta}_{td-} = 0 \quad (8)$$

Since the energy change between just before and after touchdown is calculated to be:

$$E_{td+} - E_{td-} = -\frac{MJ_l}{2(J_l + Mr_0^2)}\mu_{td-}^2, \quad (9)$$

the condition (8) means there is no energy exchange between the robot and the ground, provided no control input applied during stance phase. Having determined θ_d and $\dot{\theta}_d$, finally we can apply the same controller (6), which, in this time, becomes linear dead-beat controller.

As a result, interesting *quasi-periodic orbits* [16], which can be seen in some Hamiltonian system, are found [15]. Fig. 4 depicts such a simulation result. Herein, the free parameters of initial values are chosen to be $\theta_0 = 0.25$ [rad] and $\dot{x}_0 = 2$ [m/s] (off the fixed point). The region

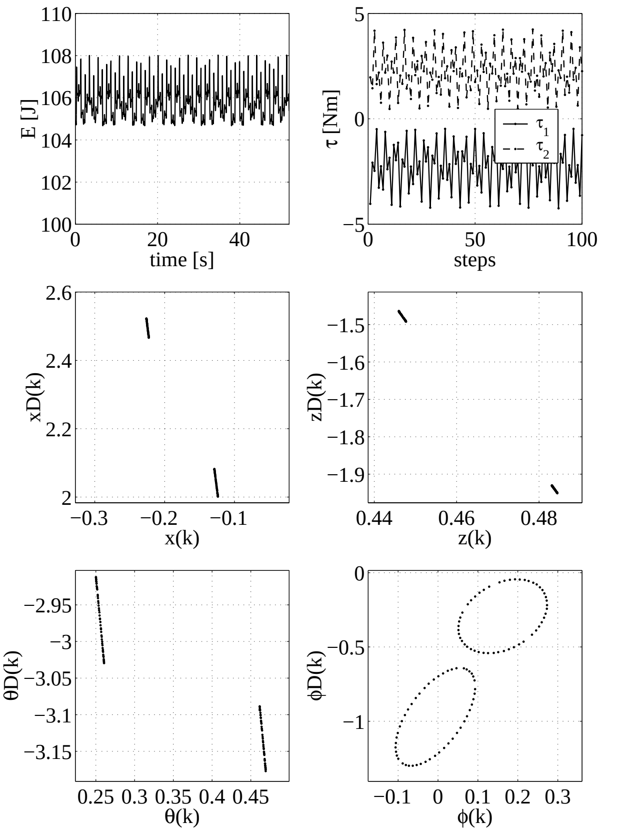

Fig. 4. Simulation result of *Energy-Preserving Touchdown Control*: The top two graph shows time evolutions of energy level (E) and control inputs (τ_1 and τ_2). The lower four graphs represent the selected images of the Poincaré map, where notation "D" represents the time derivatives of preceding variables. Please note that the position x is manually reset at each iterative crossing of the section, for visibility. Although all the points are bounded in some regions, there are no fixed points appeared. From this, we can see the gait obtained is quasi-periodic one.

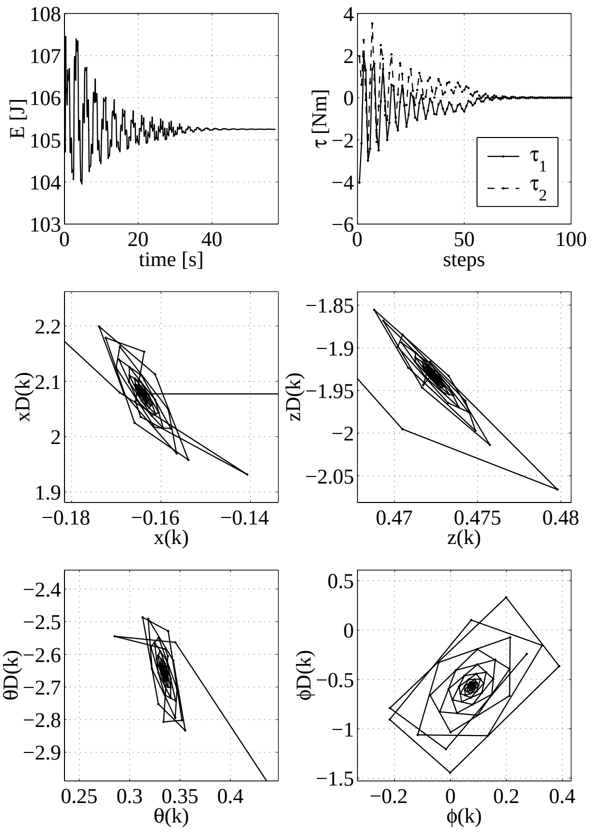

Fig. 5. Simulation results of the orbital stabilization controller and adaptive enegy controller. The top two graph shows time evolutions of energy level (E) and control inputs (τ_1 and τ_2. The lower four graphs represent the selected images of the Poincaré map, where notation "D" represents the time derivatives of preceding variables. Please note that the position x is manually reset at each iterative crossing of the section, for visibility. The input minimization via adaptive energy controller is activated from the 60th step. You can see the images of Poincaré map asymptotically converge to one fixed point and the control inputs eventually converge to zero!

of attraction is very large if we do not specify forward velocity. It is quite different point from the above local state feedback controller. Since the gaits obtained are nonlinear flows on an invariant manifold

$$\dot{E}_{sys} := \dot{E} - \tau\dot{\psi} = 0, \tag{10}$$

if there is a sudden change of energy level, the gait jumps to new quasi-periodic orbits, hence we can say the controller has some robustness against disturbance.

Thanks to the similar recurrent property between quasi-periodic orbits and chaotic orbits, we can apply a *delayed feedback*-like controllers for chaotic system [17], to asymptotically stabilize quasi-periodic gaits to (unknown) periodic ones "having desired period". Specifically, θ_d can be chosen as follows.

$$\theta_d(k) = \begin{cases} -\frac{1}{2}(\theta_{lo}(k) + \theta_{lo}(k-p)), & \text{if } k > p \\ -\theta_{lo}(k), & \text{else,} \end{cases} \tag{11}$$

where $k > 1$ is the iteration step and $p > 1$ is a desired period. A general form of delayed feedback and its limitation can be found in e.g. [18]. Note that the desired angular velocity $\dot{\theta}_d(k)$ is automatically determined by (8) accordingly. Especially for 1-periodic gait ($p = 1$), with an additional adaptive energy controller, the robot eventually hops without any control inputs, that is, complete passive running is obtained. Fig. 5 is an example of simulation results, which shows the complete passive running. The detailed description and results can be found in the literature [13].

III. BIPED RUNNING ROBOT

In this section, a planar biped running is presented. The biped model is the example that we cannot find passive solution. As described in Section I, even we cannot find any passive gaits, we may find some controllers, which generate stable limit cycle, where the control inputs can be made small enough although it cannot be zero.

A. Model

Figure 6 shows a planar biped robot considered here. The robot has two springy telescopic legs swinging around hip joints. Leg actuators are mounted parallel to the leg spring.

The generalized coordinates are defined as the position of CoG, $x = (x_g, z_g)^T \in R^2$, the attitude of the torso, $\phi \in$

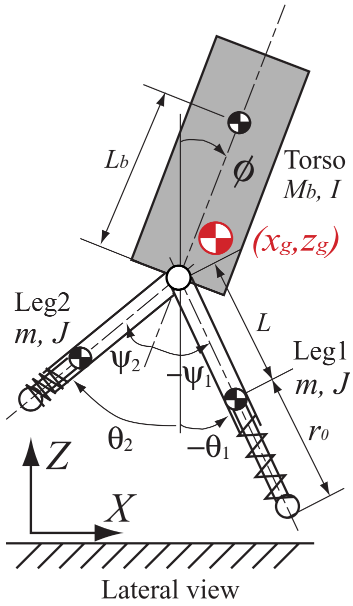

Fig. 6. Biped running robot

R^1, and joint angles, $\psi = (\psi_1, \psi_2)^T \in R^2$. Table III shows the physical parameters, together with the values used in later simulations. This model is highly nonlinear because it has massive legs and torso, whose CoG are located away the hip joint. We suppose the same assumption as one-legged case. The equations of motion are shown in [19].

B. Passive running gait searching

We have applied almost the same numerical algorithm (Fig. 2) to find passive biped running gait. Only the number of the phase is increased because the robot has two legs. Wherein, the hip springs are installed as in the case of one-legged model to make the leg swung passively. However, no passive running gaits, except for trivial solution (vertical hopping), were found. The reason seems to lie on the torso located above the hip joint. It is known that a torso mounted below the hip joint has passive stability [2]. Therefore, in contrast to one-legged robot, in which no control inputs are applied, the biped robot cannot hold its torso upright posture without pitch control, because of reaction forces from hip joints. Our analysis implies that just installing hip spring between the torso and the leg is not enough to keep the torso upright.

TABLE III
PHYSICAL PARAMETERS OF BIPED MODEL

	Meaning	Unit	Value
r_0	natural leg length	m	0.08
L	position of the leg CoG	m	0.16
L_b	position of the torso CoG	m	0.2
M_b	mass of torso	kg	4.11
m	mass of leg	kg	2.13
I	inertia of torso	kgm^2	0.05
J	inertia of leg	kgm^2	0.015
K_l	leg spring stiffness	N/m	3000

C. Stabilizing controller

In this section, we derive a controller similar to one-legged model to find stable "unknown" running gaits. First, we should overcome the instability caused by the torso at the stance phase. Here we remove hip springs and temporarily introduce simple pitch control:

$$\tau_1 = -K_{1p}\phi - K_{1d}\dot{\phi}, \tag{12}$$

where $K_{1p} \geq 0$ and $K_{1d} \geq 0$. The supporting leg is assumed to be Leg1 indicated in Fig. 6.

For swinging leg (Leg2), we are also temporarily controlling it by

$$\tau_2 = -K_{2p}(\psi_2 + \psi_1) - K_{2d}(\dot{\psi}_2 + \dot{\psi}_1). \tag{13}$$

Under this controller, counter oscillation of each leg is expected during running.

Next, we apply the controller of one-legged model to the biped at the flight phase. To do so, decoupling control and target dynamics are introduced. By new control inputs u_1 and u_2, a part of the equations of motion is decoupled:

$$\begin{bmatrix} \ddot{\psi}_1 \\ \ddot{\psi}_2 \end{bmatrix} = \begin{bmatrix} u_1 \\ u_2 \end{bmatrix} \tag{14}$$

This equation means we can control $\ddot{\psi}$ arbitrarily by new control inputs u_1 and u_2.

Next, we define a target dynamics. Conservation law of the angular momentum around CoG can be expressed as

$$J_0\dot{\phi} + J_1\dot{\psi}_1 + J_2\dot{\psi}_2 = P_0, \tag{15}$$

where $J_i (i = 0, 1, 2)$ is nonlinear inertia terms and P_0 means initial angular momentum of flight phase. If we chose

$$\dot{\psi}_2 = \frac{1}{J_2}(P_0 - J_0\dot{\phi}_0 - J_1\dot{\psi}_1) \tag{16}$$

($\dot{\phi}_0$ is the initial value of $\dot{\phi}$ at flight phase), we get the following target dynamics.

$$\dot{\phi} \;=\; \dot{\phi}_0 \tag{17}$$

This means "another first integral of motion is created by a feedback control". The control input u_2 can be calculated by combining (16) and the original equations of motion.

The final task is to determine the control input u_1. The control objective is to dead-beat the absolute angle of the swing leg θ_1 and its velocity $\dot{\theta}_1$ to some desired values at given fixed time T_v (flight time). As we explained in Section II, desired values are chosen to preserve energy at touchdown. For the biped robot case, condition of energy preservation is given by:

$$\hat{\lambda}_p = 0, \tag{18}$$

where $\hat{\lambda}_p$ is the constraint impulse imposed at touchdown, which can be calculated explicitly.

For a given flight time T_v, however, there are many pairs of θ_d and $\dot{\theta}_d$, as in the case of one-legged model. To find "unknown" periodic running gait, we set θ_d according to (11). Since (14) is a trivial second order linear ODE, we can easily dead-beat ψ_1 and $\dot{\psi}_1$, by applying the same controller as (6) to u_1.

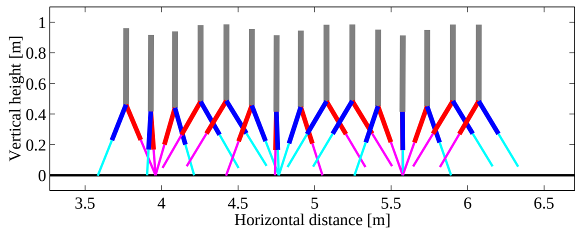

Fig. 7. Stick animation of subsequent three steps of 1-periodic biped running, corresponding to Fig. 8. The robot moves from left to the right.

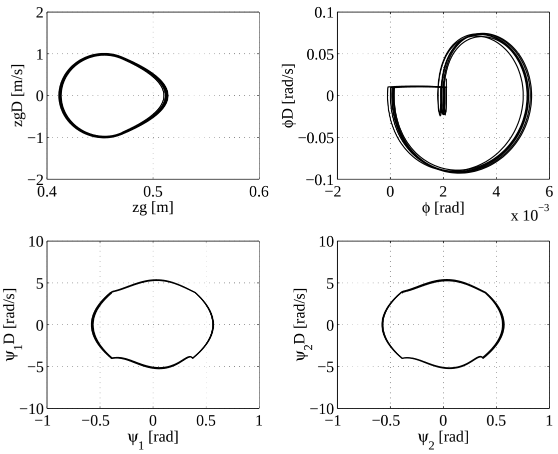

Fig. 8. Phase portraits of stable 1-periodic running gait of 2 m/s in horizontal speed, where the control parameters are $K_{p1} = 200, K_{d1} = 50, K_{p2} = 100, K_{d2} = 10$. Notation "$D$" represents the time derivatives of preceding variables. Note that the scale of the abscissa of right top is 10^{-3} and small horizontal curve running form $\phi = 0$ [rad] to 2×10^{-3} [rad] does not mean an instantaneous jump, but indicates the result of high-gain PD-feedback about body pitch.

D. Simulation

Using the above controller, stable one-periodic running gaits are investigated. Fig. 7 shows the stick animation of 2 m/s running and Fig. 8 depicts the corresponding phase portraits. Stable running in different horizontal speed is also obtained. Interestingly, dynamics about Leg2 (zero dynamics of decoupling controller) is found to be stable. Actually, the motion of Leg2 indicates the counter oscillation to Leg1. Although the running gait seems to have symmetry, the motion of torso is slightly asymmetry, as recognized from the right top graph of Fig. 8. This asymmetry become more significant if the feedback gains of (12) become smaller. Without attitude control, the robot falls down after a few steps. Stabilization to (unknown) period 2 gaits ($p = 2$) is also succeeded [19].

IV. Quadruped Running Robot

In this section passive running of a planar quadruped robot is presented. Gait searching becomes more complicated than one-legged case and only the outline is shown.

A. Model

The model of a planar quadruped robot is shown in Fig. 9. This is the extended model of Fig. 1. That is, it has springy telescopic legs rotating around hip joint with hip springs. All of the assumptions are the same as those in the one-legged or the biped. The physical parameters are summarized in Table Table IV.

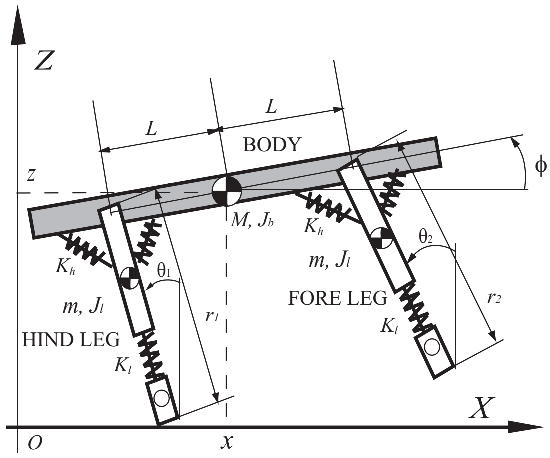

Fig. 9. Planar quadruped running robot

TABLE IV
PHYSICAL PARAMETERS OF QUADRUPED MODEL

	Meaning	Unit	Value
r_0	natural leg length	m	0.5
L	distance between the legs	m	0.4 or 0.25 *
M_b	mass of torso	kg	20
m	mass of leg	kg	1 or 3 *
J_b	inertia of torso	kgm^2	1.67
J_l	inertia of leg	kgm^2	0.017 or 0.051 *
K_l	leg spring stiffness	N/m	8000
K_h	hip spring stiffness	Nm/rad	25

* L, m and J_l differ for each Profile A or B (Fig. 14).

The model can be completely described by 7 co-ordinates, we define a generalized coordinate $q = [\theta_1\ \theta_2\ \phi\ x\ y\ r_1\ r_2]^T$ and the state vector $\bar{x} = [q\ \dot{q}]^T$, where (θ_1, θ_2) are the leg angles, ϕ is the pitch angle, (x, y) are the Cartesian coordinates of the body's CoG, and (r_1, r_2) are the length of the fore and hind leg respectively.

Note that in planar quadruped model, each pair of fore legs and hind legs moves together, and hence, only the bounding gaits can be generated (gallop does not appear). A complete bounding cycle is showed in Fig. 10. We can see from the figure that each of these events initiates the corresponding phase.

Related to the quadruped passive running, there is a preceding study [21]. The main differences of our model to their model are; consideration of mass of legs and hip springs. As described in Section I, the important physical phenomena that flowed from this consideration are: passive swinging of the leg, the counter-oscillatory motion of the body, and energy-loss due to the impact between the foot and the ground.

The equation of motion is represented by the following set of differential equations and algebraic equations:

- Continuous dynamics:

$$\dot{\bar{x}} = f_i(\bar{x}) \quad (i = 1, \cdots, 4) \tag{19}$$

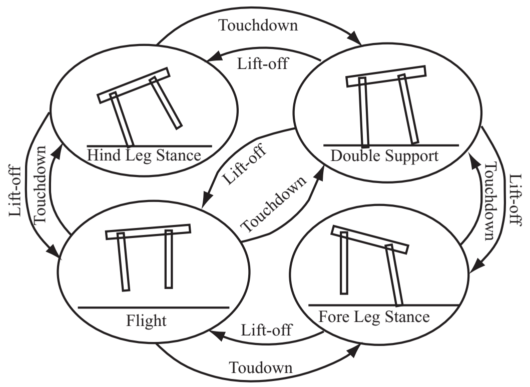

Fig. 10. Phase transition of planar quadruped running gait

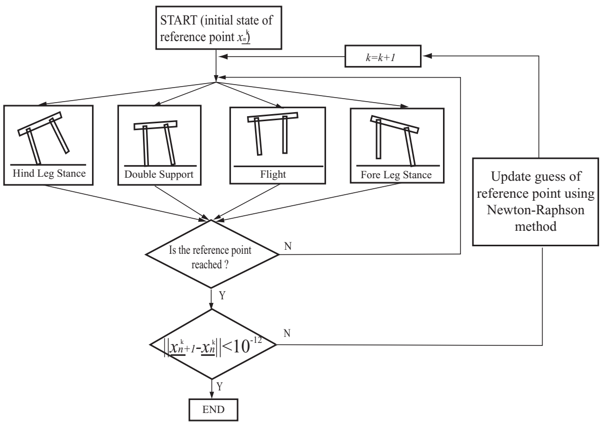

Fig. 11. Gait searching algorithm for quadruped model

- Discrete dynamics:

$$\bar{x}_+ = H_j(\bar{x}_-) \quad (j = 1, \cdots, 4) \tag{20}$$

Here, $f_{1,2,3,4}$ the vector fields corresponds to each phase Hind Leg Stance, Double Support, Fore Leg Stance, Flight respectively. $H_{1,2,3,4}$ corresponds to events Hind Leg Touchdown, Fore Leg Touchdown, Hind Leg Lift-off, Fore Leg Lift-off, respectively. The details of equations are given in [20] and will be published elsewhere.

In continuous phase, the equation of motion can be represented by four different dynamical system, which takes the form of autonomous system because we have no inputs. Note that the DOF of each phase is different and they are all bellow 7. Therefore, some of the variables in the vector $\bar{x}$, do not participate in the dynamic equations in some phases. In this case, they become the dependent variables, and the update of these variables should be calculated based on the constraints subjects to the corresponding phases.

On the other hand, the equation of motion at transition phase can be represented by four different algebraic equations. The transition models mainly contribute to describe the behavior of the impact phenomena, which occurs when the leg strikes the ground (the other is to describe "reset" of the position at the end of one stride). This consideration complicates the analysis greatly. However, they are expected to be a more realistic system description.

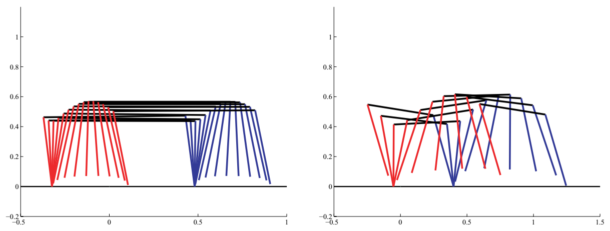

(a) Gait A (b) Gait B

Fig. 12. Two different passive running gaits: the hind leg touches the ground in Gait A, while the fore leg touchdowns first in Gait B.

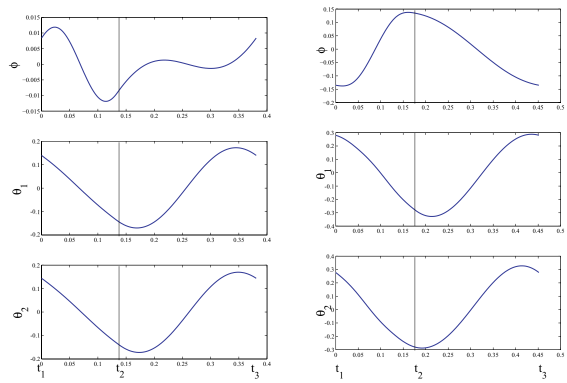

(a) Gait A (b) Gait B

Fig. 13. Time trajectories of one stride of running: The graphs imply the symmetry; $\phi(t_1) = -\phi(t_2) = \phi(t_3)$, $\theta_1(t_1) = -\theta_1(t_2) = \theta_1(t_3)$ and $\theta_2(t_1) = -\theta_2(t_2) = \theta_2(t_3)$

B. Passive running gaits

Since the quadruped running is composed of multiple phases, an advanced algorithm is implemented as shown in Fig. 11, where no order of phase transition is presumed. Depending on which event occurs, the integrator selects the appropriate equations of motion, which correspond to the phase triggered by that event according to Fig. 10. The fixed point to be found is $\underline{x}^* = [\theta_1^*, \theta_2^*, \phi^*, \dot{\theta}_1^*, \dot{\theta}_2^*, \dot{\phi}^*, \dot{r}_1^*]$ at the cross section of poincaré map selected as the event of Hind Leg Touchdown, or $\underline{x}^* = [\theta_1^*, \theta_2^*, \phi^*, \dot{\theta}_1^*, \dot{\theta}_2^*, \dot{\phi}^*, \dot{r}_2^*]$ at Fore Leg Touchdown. Although we do not assume any specific order of phase transition, only the gaits which tend to converge will exhibit a repetition of ordered phases. Thanks to this algorithm, two typical gaits, Gait A and Gait B, shown in Fig. 12(a) and Fig. 12(b) respectively, are obtained. In Gait A, the Hind Leg Touchdown event occurs first after Flight, while in Gait B, the Fore Leg Touchdown event occurs first. From their analysis, the followings are concluded.

First, different from other related studies, all the passive running gaits we found are proved to be unstable. The investigation of characteristic multipliers corresponding to the periodic gaits revealed that their magnitude are outside the unit circle. For example, Gait A is the periodic orbit with the fixed point $\underline{x}^* = [0.1396, 0.1438,$

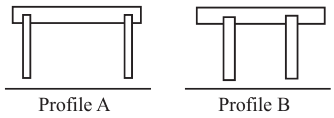

Fig. 14. Two different profiles

0.0084, -1.7619, -1.5909, 0.2482, -1.4232], whose characteristic multiplier $\mathrm{eig}(DP)|_{\underline{x}^*}$ is [7.1516, -0.7776, -0.1961+0.3112i, $-0.1961 - 0.3112i$, 0.2130, 0.0567, 0.0018] and Gait B is the periodic orbit with the fixed point $\underline{x}^* =$ [0.2800, 0.2778, -0.1350, -0.9629, -2.5999, -0.3145, -1.8308], where $\mathrm{eig}(DP)|_{\underline{x}^*}$ is [-7.3902, 1.5585, -0.8970, -0.7272, -0.0019, $-0.2030 + 0.0901i$, $-0.2030 - 0.0901i$]. Although the motion starting from the fixed points can continue for some steps (8 and 25 steps as maximum for Gait A and B respectively), it falls finally.

Secondly, our simulations reveal that both Gait A and Gait B exhibit symmetric behavior. The time evolution of angles shown in Fig. 13(a) or Fig. 13(b) implies such symmetric properties: $\phi(t_1) = -\phi(t_2) = \phi(t_3)$, $\theta_1(t_1) = -\theta_1(t_2) = \theta_1(t_3)$ and $\theta_2(t_1) = -\theta_2(t_2) = \theta_2(t_3)$. This property agrees with the result of [21].

Thirdly, thre is a strong profile dependency of passive running gaits. Actually, Gait A and Gait B are generated by two different profile (Table 9, Fig. 14). In our numerical analysis, Profile A always converges to Gait A, and Profile B always converges to Gait B.

V. Conclusion

We reported on passive running of planar one-legged, biped, and quadruped robot. The robots are installed with linear springs at the telescopic knee joints and torsional springs at the hip joints. In this paper we addressed the analysis of passive running gaits and their orbital stabilization.

For a planar one-legged robot, passive running gaits were found numerically. To this end, numerical search algorithm was introduced. The analysis showed that the all passive running gaits were unstable except for a trivial gait. Next, orbital stabilizing controller was derived, based on energy-preserving principle. Different from a local feedback controller derived from the linearized Poincaré map, the new controller demonstrated the best harmony with the passive gaits. With this controller, interesting quasi-periodic orbits, which can be seen in Hamiltonian system, were observed. Moreover, with an additional adaptive scheme similar to delayed feedback in chaotic system, orbitaly stabilization to (unknown) passive running gaits were achieved and the control inputs converged to zero.

For a planar biped robot attached with torso above hip joint, we could not find any periodic passive solution. Nevertheless, with a simple attitude controller at stance phase and delayed feedback-like controller in flight phase, “almost symmetric” stable 1-periodic running gaits were generated.

For a planar quadruped robot, more advanced numerical algorithm was developed. With this algorithm, two typical different passive running gaits were found. Although the results are premature, we found the following properties of the passive running gaits: Firstly they were all unstable except for trivial case, secondly they had symmetry, thirdly they had a strong profile dependency.

Our ongoing task includes continual searching and analysis of passive running gaits for both of the biped and the quadruped. The experiments with biped robot are also performed in parallel.

Acknowledgement

This research was partially supported by the Ministry of Education, Science, Sports and Culture, Grant-in-Aid for Young Scientists, 15760144, 2003.

References

[1] M. Raibert: *Legged Robots That Balance*, MIT Press, 1985.
[2] G. Zeglin and B. Brown: ”Control of a bow leg hopping robot”, Proc. of IEEE ICRA, pp.793–798, 1998.
[3] U. Saranli, M. Buehler and D.E. Koditschek: ”RHex: a simple and highly mobile hexapod robot,” Int. J. Robotics Research, vol.20, no.7, pp.616–631, 2001.
[4] Y. Fukuoka, H. Kimura, et al.: ”Adaptive dynamic walking of a quadruped robot ’Tekken’ on irregular terrain using a neural system model”, Proc. of IEEE ICRA, pp.2037–2042, 2003.
[5] S. Hyon and T. Mita: ”Development of a biologically inspired hopping robot –“Kenken””, Proc. of IEEE ICRA, pp.3984-3991, 2002.
[6] R. M’Closkey and J. Burdick: ”Periodic motions of a hopping robot with vertical and forward motion”, Int. J. Robotics Research, vol.12, no.3, pp.197–218, 1993.
[7] W. Schwind and D. Koditschek: ”Control of forward velocity for a simplified planar hopping robot”, Proc. of IEEE ICRA, pp.691–696, 1995.
[8] R. Altendorfer, D. E. Koditschek and P. Holmes: ”Toward factored analysis of legged locomotion models”, Proc. of IEEE ICRA, pp.37–44, 2003.
[9] C. Thompson and M. Raibert: ”Passive dynamic running”, Experimental Robotics I, eds. V.Hayward and O. Khatib., pp.74-83, Springer, 1989.
[10] M. Ahmadi and M. Buehler: ”Stable control of a simulated one-legged running robot with hip and leg compliance”, IEEE Trans. on Robotics and Automation, vol.13, no.1, pp.96–104, 1997.
[11] M. Ahmadi and M. Buehler: ”The ARL Monopod II running robot: control and energetics”, Proc. of IEEE ICRA, pp.1689–1694, 1999.
[12] C. François and C. Samson: ”A new approach to the control of the planar one-legged hopper”, Int. J. Robotics Research, vol.17, no.11, pp.1150–1166, 1998.
[13] S. Hyon and T. Emura: ”Energy-preserving control of passive one-legged running robot”, Advanced Robotics, vol.18, no.4, 2004 (to be published).
[14] T. Kousaka, T. Ueta and H. Kawakami. Bifurcation of switched nonlinear dynamical systems. IEEE Trans. Circuits and Systems II, vol.CAS-II, no.7, pp.878–885, 1999.
[15] S. Hyon and T. Emura: “Quasi-periodic gaits of passive one-legged hopper”, Proc. of IEEE/RSJ IROS, pp.2625-2630, 2002.
[16] Arnold: *Mathematical Methods of Classical Mechanics*, Springer, 1978.
[17] K. Pyragas: ”Continuous control of chaos by self-controlling feedback”, Physi. Lett., A 170, pp.421–428, 1992.
[18] T. Ushio: ”Limitation of delayed feedback control in nonlinear discrete-time systems”, IEEE Trans. Circuits and Systems I, vol.43, pp.815–816, 1996.
[19] S. Hyon and T. Emura: ”Running control of a planar biped robot based on energy-preserving strategy”, Proc. of IEEE ICRA, 2004 (to be published).
[20] X. Jiang: ”A study on passive quadruped running robot”, MS thesis, Tohoku University, March 2004.
[21] I. Poulakakis, J. Smith and M. Buehler: ”On the stable passive dynamics of quadrupedal running”, Prof. of IEEE ICRA, pp.1368–1373, 2003.